# REPORT DOCUMENTATION PAGE

*Form Approved*
*OMB No. 0704-0188*



**1. REPORT DATE** *(DD-MM-YYYY)*
16-02-2007

**2. REPORT TYPE**
Final Technical

**3. DATES COVERED** *(From - To)*
1 Apr 2004 - 31 Dec 2006

**4. TITLE AND SUBTITLE**
Fundamental Physics and Practical Applications of
Electromagnetic Local Flow Control in High Speed Flows

**5a. CONTRACT NUMBER**

**5b. GRANT NUMBER**
FA9550-04-1-0177

**5c. PROGRAM ELEMENT NUMBER**

**6. AUTHOR(S)**
Knight, D., Yan, H., Candler, G., Glumac, N., Elliott, G., and Zheltovdov, A.

**5d. PROJECT NUMBER**

**5e. TASK NUMBER**

**5f. WORK UNIT NUMBER**

**7. PERFORMING ORGANIZATION NAME(S) AND ADDRESS(ES)**
Dept of Mechanical and Aerospace Engineering
Rutgers University
98 Brett Road
Piscataway, NJ 08854-8058

**8. PERFORMING ORGANIZATION REPORT NUMBER**
CCD 2007-1

**9. SPONSORING / MONITORING AGENCY NAME(S) AND ADDRESS(ES)**
Air Force Office of Scientific Research
AFOSR/NA Dr John Schmisseur
875 North Randolph St
Suite 325, Rm 3112
Arlington, VA 22203

**10. SPONSOR/MONITOR'S ACRONYM(S)**

**11. SPONSOR/MONITOR'S REPORT NUMBER(S)**

**12. DISTRIBUTION / AVAILABILITY STATEMENT**
Unclassified; Distribution Unlimited

AFRL-SR-AR-TR-07-0135

**13. SUPPLEMENTARY NOTES**

**14. ABSTRACT**
Achievement of the future US Air Force mission requires development of new high speed air vehicles. The aerodynamic performance of high speed air vehicles is sensitive to *local* flow phenomena which may adversely affect vehicle operation and possibly result in vehicle loss. An example is the Edney IV shock-shock interaction which causes intense local surface heat transfer. New concepts in local flow control for high speed flows are needed to alleviate or eliminate adverse local flow phenomena. Recently, a promising new research field in local flow control for high speed flows has emerged - Electromagnetic Local Flow Control (ELFC). Examples include beamed energy addition (*e.g.*, laser and/or microwave energy deposition) and DC discharge, with or without external magnetic fields. Recent conferences and workshops have emphasized the importance of ELFC and identified many promising opportunities. This report describes the research accomplishments of Rutgers - The State University of New Jersey, the University of Illinois Urbana-Champaign and the University of Minnesota in understanding the fundamental physics and practical applications of Electromagnetic Local Flow Control in high speed flows.

**15. SUBJECT TERMS**
Plasmadynamics, gas dynamics, supersonic flow, aerodynamics, computational fluid dynamics, real gases, vortex dynamics, microwave

| 16. SECURITY CLASSIFICATION OF: | | | 17. LIMITATION OF ABSTRACT | 18. NUMBER OF PAGES | 19a. NAME OF RESPONSIBLE PERSON |
|---|---|---|---|---|---|
| | | | | | Doyle Knight |
| **a. REPORT** | **b. ABSTRACT** | **c. THIS PAGE** | UU | 14 | **19b. TELEPHONE NUMBER** *(include area code)* |
| U | U | U | | | 732 445 4464 |

FUNDAMENTAL PHYSICS AND PRACTICAL APPLICATIONS OF ELECTROMAGNETIC LOCAL FLOW CONTROL IN HIGH SPEED FLOWS

AFOSR GRANT FA9550-04-1-0177


Doyle Knight and Hong Yan
Department of Mechanical and Aerospace Engineering
Rutgers - The State University of New Jersey

Greg Elliott[†] and Nick Glumac[††]
[†]Department of Aeronautical and Astronautical Engineering
[††]Department of Mechanical and Industrial Engineering
University of Illinois at Urbana-Champaign

Graham Candler
Department of Aerospace Engineering and Mechanics
University of Minnesota

Alexander Zheltovodov
Institute of Theoretical and Applied Mechanics
Novosibirsk, Russia


Submitted to:

Dr. John Schmisseur
Air Force Office of Scientific Research
875 North Randolph Street
Suite 325, Room 3112
Arlington, VA 22203
Phone: 703 696 6962 · Fax: 703 696 8451
Email: John.Schmisseur@afosr.af.mil


February 16, 2007

**Abstract**

Achievement of the future US Air Force mission requires development of new high speed air vehicles. The aerodynamic performance of high speed air vehicles is sensitive to *local* flow phenomena which may adversely affect vehicle operation and possibly result in vehicle loss. An example is the Edney IV shock-shock interaction which causes intense local surface heat transfer. New concepts in local flow control for high speed flows are needed to alleviate or eliminate adverse local flow phenomena.

Recently, a promising new research field in local flow control for high speed flows has emerged - Electromagnetic Local Flow Control (ELFC). Examples include beamed energy addition (*e.g.*, laser and/or microwave energy deposition) and DC discharge, with or without external magnetic fields. Recent conferences and workshops have emphasized the importance of ELFC and identified many promising opportunities.

This report describes the research accomplishments of Rutgers - The State University of New Jersey, the University of Illinois Urbana-Champaign and the University of Minnesota in understanding the fundamental physics and practical applications of Electromagnetic Local Flow Control in high speed flows.

## I. Introduction

The overall research objectives are 1) develop and validate improved models of unsteady laser, microwave and combined laser/microwave energy deposition in air, 2) construct a new experimental facilities at the University of Illinois for investigation of laser, microwave and combined laser/microwave energy deposition in supersonic flows, and 3) evaluate the capability of unsteady laser, microwave and combined laser/microwave energy deposition for specific local flow control applications in supersonic flows.

## II. Develop and Validate Improved Models of Laser Energy Deposition in Air

### *II.A Experimental Investigation of Laser Energy Deposition in Air*

Although laser induced optical breakdown in a gas has been studied for over forty years (see, for example, Raizer[1]), there are at least two significant gaps in our knowledge, namely, 1) the temperature and electron number density at very early times, and 2) the flowfield structure subsequent to the laser spark. Our research effort focused on filling this gap in knowledge in order to achieve a full understanding of laser induced optical breakdown and to provide experimental data for validation of our theoretical models.

Temperature and electron density measurements were performed using time-resolved emission spectroscopy. A Spectra Physics GCR 230 laser (532 nm, 10 ns pulse) was used to create the optical breakdown in air at ambient temperature. The focal length was varied from 50 to 100 mm. Emission from the focal volume was imaged onto the inlet slit of an SPEX M270 imaging spectrometer (270 mm focal length) by an achromat (50 mm diameter, 100 mm focal length) at unit magnification at selected axial locations along the beam direction. The ICCD permits time resolution as small as 40 ns. The Stark-broadened spectrum was fit to a temperature and number density using an atomic spectrum modeling program.

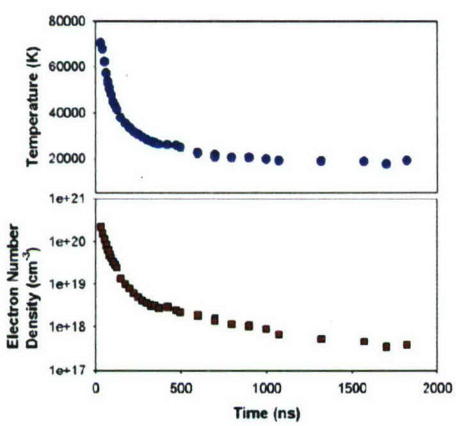


Fig. 1 Temperature and electron density as function of time at a fixed point

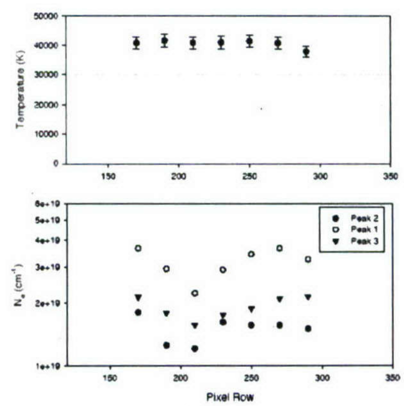


Fig. 2 Temperature and electron density as a function of distance at fixed time

---

[1] Raizer, Y., *Laser-Induced Discharge Phenomena*, Consultants Bureau, NY, NY, 1977

Temperature and electron number densities for a typical laser spark are shown in Fig. 1. The experimental uncertainty is approximately ±10% in temperature and ±50% in electron number density. The highest temperature is approximately 70,000 K and falls exponentially within the first few hundred nanoseconds with a decay constant of approximately 60 ns. After approximately 500 ns, a slower temporal decay occurs with a time constant of approximately 370 ns. The electron density immediately following the laser pulse is in excess of $10^{20}$ $cm^{-3}$, and thereafter decays with a $t^{-1.7}$ dependence up to two microseconds. After one microsecond, the electron density has decreased by two orders of magnitude.

Fig. 2 displays the temperature and electron number density along the beam axis at 150 ns following the laser pulse. Although there is significant variation in the measured intensity along the beam axis, the temperature is relatively constant. The electron density appears to show a systematic variation along the beam axis. Fig. 3 shows the temperature field measured by Filtered Rayleigh Scattering at four different times after the laser spark. The uncertainty in the temperature measurement is ±8%. The temperature with the heated region varies from 3000 K (red) to 1000 K (blue). The decay of the maximum temperature follows an exponential curve with a time constant of 24.4 microseconds.

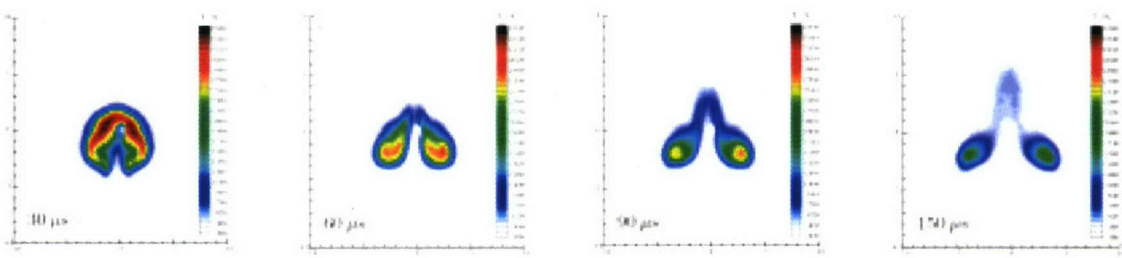

Fig. 3 Temperature field of laser spark measured by Filtered Rayleigh Scattering

A detailed investigation was conducted on the effect of ambient pressure in the range of 0.1 atm to 1.0 atm on the size, temperature, electron number density, and fraction of laser energy absorbed in a laser-induced plasma in air. A facility for conducting controlled laser discharge experiments under controlled atmospheric conditions was constructed. The study found that as pressure is reduced the size of the plasma, the electron number density, peak emission intensity, and the fraction of incident laser energy that is absorbed all decrease significantly. At 0.1 atm, the laser energy absorbed in the discharge is less than 5% of the incident laser power under our conditions. Normalizing the electron number density $N_e$ at each time interval by the $N_e$ at 1 atm (see Fig. 4),

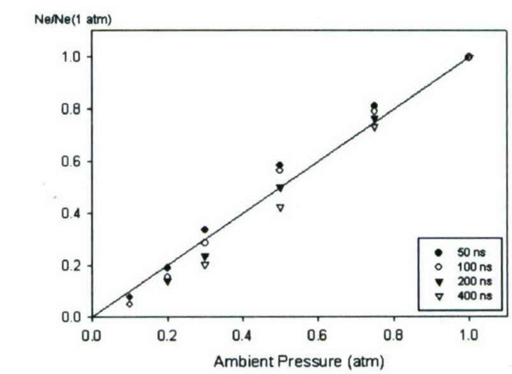


Fig. 4 $N_e$ for different times normalized by $N_e$ for the 1 atm case the ratio varies approximately linearly with ambient pressure, suggesting that the plasma number density – at least for the period of 50 to 1000 ns – scales roughly linearly with initial density for constant input laser energy. The temporal temperature profile in the plasma and the fraction of the absorbed laser energy that is converted to thermal energy in the plasma were found to remain constant, at least down to 0.2 atm. The geometry of the plasma was measured from instantaneous emission images over the full range of pressures and time. In addition to the bimodal appearance of the spark for all cases it was found that at higher pressures the breakdown initiates at a location slightly before the focal point of the lens with the region of highest emission propagating toward the incoming laser beam. As the pressure decreases below 0.5 atm, however, the laser spark originates from a central point and propagates more symmetrically. This change in the propagation characteristics of the emission with pressure may suggest that multi-photon ionization is dominant at lower pressures (Bindhu *et al*[2]).

*II.B Simulation of Laser Energy Deposition in Air*

A real gas model of laser energy deposition in air, initially developed under previous AFOSR support, was further evaluated by comparison with experiments conducted at the University of Illinois for different values of input laser energy and focal length of the converging lens. The model incorporates eleven species ($N_2$, $O_2$, NO, N, O, $N_2^+$, $O_2^+$, $NO^+$, $N^+$, $O^+$ and *e*), a chemical kinetics model for three temperature air (translational-rotational, vibrational and electron temperatures) developed at Stanford University[3] and a model for adsorption and reflection of the incident laser energy pulse (Fig. 5). The absorption and reflection parameters of the model were previously determined by matching the experimental growth of the radius of the blast wave *vs* time generated by a laser pulse in air within incident energy $E_o = 108$ mJ at a focal length $f = 100$ mm.

Fig. 6 shows the results of four simulations performed for a laser pulse of higher incident energy $E_o = 180$ mJ at the same focal length $f = 100$ mm using different values of the characteristic cross-section of adsorption $Q$. The computed value of the adsorbed energy $E_{abs}$ for the calibrated value $Q_o$ is 150 mJ in close agreement with the experimental value of 151 mJ. The model was further extended to a range of ambient pressures and lens focal lengths. The model was recalibrated and extensive comparisons to experimental data were made. The reflectivity and absorptivity were re-calibrated through detailed comparisons with experimental data from the University of Illinois obtained under this grant. The

---

[2] Bindhu, C., Harilal, S., Tillack, M., Najmabadi, F. and Gaeris, A., "Laser Propagation and Energy Absorption by an Argon Spark", *Journal of Applied Physics*, Vol. 94, 2003, pp. 7402-7407.

[3] Laux, C., Pierrot, L., Gessman, R., and Kruger, C., "Ionization Mechanisms of Two-Temperature Plasmas", AIAA Paper No. 99-3476, June 1999.

model captured the critical feature that the laser energy deposition region grows toward the laser during the laser pulse.

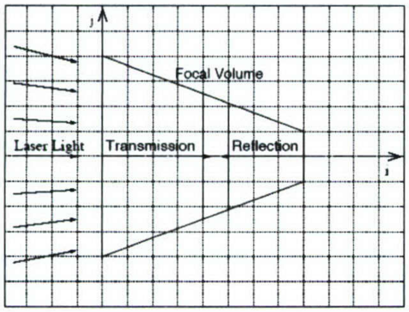


Fig. 5 Model for adsorption and radiation

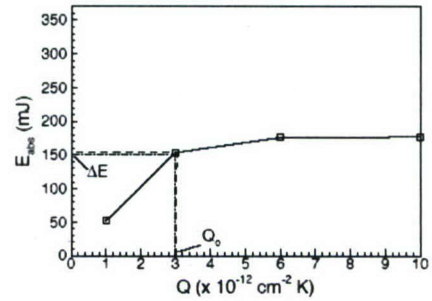


Fig. 6 Computed energy adsorption *vs* adsorption coefficient *Q*

*II.C Kinetic Model for Simulation of Microwave Energy Deposition in Air*

A kinetic model for simulation of microwave energy deposition in air was developed in collaboration with Drs. D. Khmara, Y. Kolesnichenko, V. Brovkin (Institute of High Temperatures [IVTAN], Moscow, Russia) and Drs. V. Lashkov and I. Mashek (St. Petersburg State University, St. Petersburg, Russia). The model includes 23 species and 256 reactions. The model for gas heating incorporates the effects of elastic collisions of electrons, heat of reactions and rotational heating through microwave energy deposition. A simulation of microwave energy deposition in air was performed for specific experimental conditions at IVTAN. The initial concentrations of $N_2$ and $O_2$ corresponded to a pressure $p = 70$ Torr and gas temperature $T_g$ = 200K. The microwave frequency was 9 GHz and the pulse duration was 1.8 μs. The measure electric field $E$ *vs* $t$ (Fig. 7) was specified for the computations. The computed gas temperature $T_g$ *vs* $t$ is shown in Fig. 8. The computed gas temperature at 3.6μs is $T_g$ = 280 K and is in close agreement with the measured $T_g$ = 270 K based on a fit of the emission of bands 0-3 and 1-4 of the nitrogen second positive system.

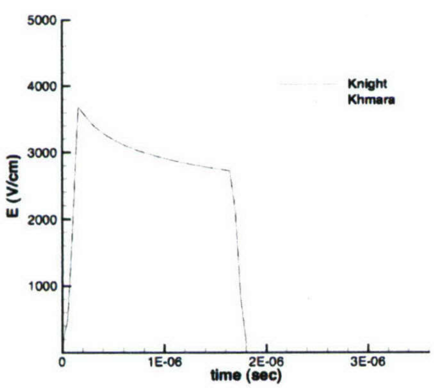


Fig. 7 $E$ *vs* $t$

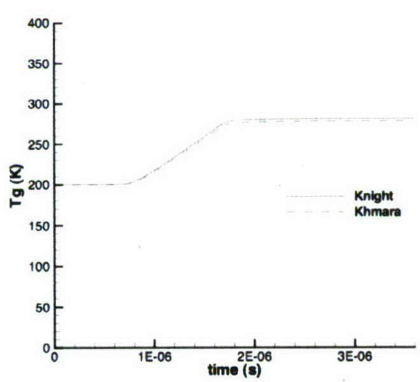


Fig. 8 $T_g$ *vs* $t$

## III. New Experimental Facilities

### *III.A Supersonic Wind Tunnel to Study Energy Deposition for Control of Normal Shock and Resonant Pressure Fluctuations in Flow Over an Open Cavity*

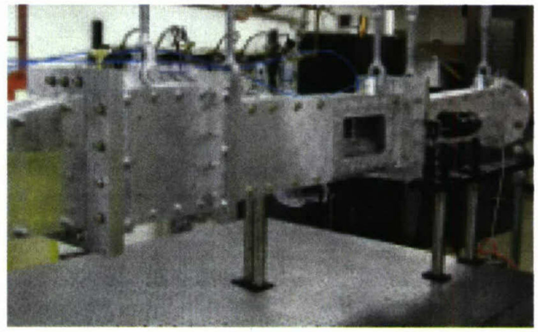

Fig. 9 Supersonic wind tunnel

A new supersonic wind tunnel to study the effects of energy deposition on normal shock waves and the supersonic flow over a two dimensional cavity was been designed, constructed. Fig. 9 shows a picture of the new facility. The wind tunnel has a 2.5 in × 2.5 in test section with excellent optical access on the top and side walls. The windows extend below the wind tunnel floor so that measurements can be taken within the two dimensional cavity. Measurements indicate that the converging diverging nozzle results in a Mach number between 1.35 and 1.4. The tunnel is supplied by a 4800 $ft^3$ tank farm pressurized by two 1200 cfm compressors (with maximum pressures of 110 and 140 psi) allowing almost continuous run times. Tests indicate that the tunnel starts at a minimum stagnation pressure of approximately 23 psia. The facility was used for the investigation of the effects of energy deposition on a normal shock and on the supersonic flow over a two dimensional supersonic cavity (see Sections IV.A and IV.B).

### *III.B Coaxial Resonator Microwave System*

A unique microwave discharge system was designed and fabricated with Gerling, Inc., and installed at the University of Illinois Urbana-Champaign (Fig. 10). The system is based upon the concept of a quarter-wave resonator, which is extremely versatile and can operate easily at elevated pressures as demonstrated by Linkenheil, Ruoß, and Heinrich[4] who have reported reliable operation at 6 atm in air. For the UIUC system continuous plasmas are can be formed in air at 1 atm. In addition to CW operation, the system was designed with pulsed capability to produce repetition rates on the order of 10 kHz. Fig. 11 shows the nondimensionalized intensity of a single pulse in a series of plasma pulses occurring at 10 kHz for atmospheric and vacuum ambient conditions in the chamber. The pulse width of the measured emission from the plasma is reduced from approximately 28μs (FWHM) to 500 ns as the ambient pressure is increased from 0.1 to 1 atm. Testing is currently underway to determine the minimum pulse width and maximum repetition rate of the current system and to develop arrangements to control the location and shape of the plasma. Also we are investigating the possible coupling between a laser-initiated spark and the microwave plasma.

---

[4]Linkenheil, K., Ruoß, H.-O., and Heinrich, W., "Design and Evaluation of a Novel Spark-Plug Based on a Microwave Coaxial Resonator," 34th European Microwave Conference, Amsterdam, pp. 1561-1564, 2004

Fig. 10. University of Illinois Urbana-Champaign Microwave coaxial resonator facility.

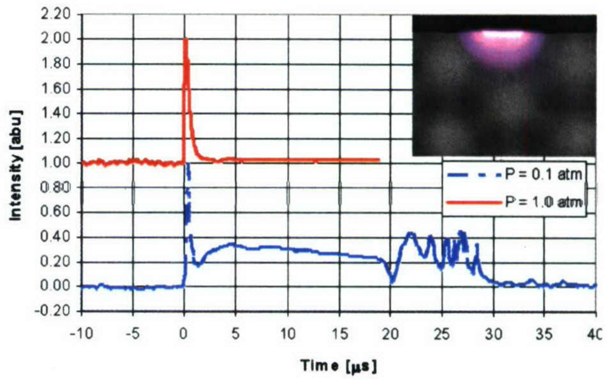


Fig. 11. Traces of the emission from a pulsed plasma formed from a microwave coaxial resonator. Inset: Photo of plasma at 0.1 atm.

## IV. Evaluate Capability for Local Flow Control

### *IV.A Control of Normal Shock*

Control of the location of the terminal (quasi-normal) shock in a mixed compression inlet (Fig. 12) is critical to maintaining inlet performance and stability. The total pressure recovery of the inlet is strongly dependent on the location of the terminal shock which accounts for most of the total pressure loss in the inlet. The design location for the terminal shock involves a tradeoff between performance and stability. As the terminal shock is positioned closer to the inlet (aerodynamic) throat, the inlet total pressure recovery increases while the terminal shock stability decreases. Movement of the terminal shock upstream of the inlet (aerodynamic) throat due to gust response or engine-generated acoustic perturbations leads to expulsion of the terminal shock from the inlet ("unstart") and a drastic decrease in total pressure recovery.

The capability for control of the location of a terminal (normal) shock by laser energy deposition has been examined using perfect gas and real gas models developed in this research. The configuration, shown in Fig. 13, is a converging-diverging nozzle with a second throat to position a normal shock at a fixed location with the test section (region AB).

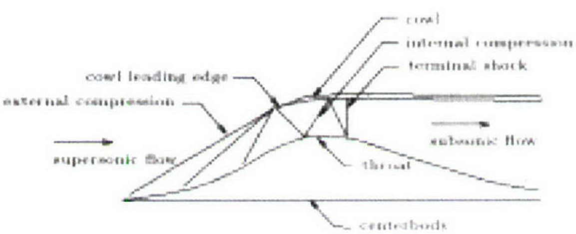


Fig. 12 Mixed compression supersonic inlet

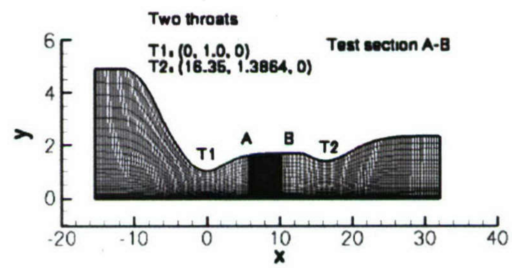


Fig. 13 Computational domain for shock

An example of results are presented in Figs. 14 and 15 for a laser pulse with dimensionless energy $\varepsilon = 100$ where $\varepsilon = E_{abs}/\rho_\infty c_p T_\infty V$ where $E_{abs}$ is the energy deposited in volume $V$ at time $t = 2.5$ nondimensionalized by $H/U_\infty$ where $H$ is the half-height of the channel at the location of the normal shock and $U_\infty$ is the freestream velocity. The freestream conditions are Mach number $M_\infty = 2$, $T_\infty = 157$ K and $\rho_\infty = 0.667$ kg/m$^3$. The laser pulse causes a substantial upstream deformation of the shock which would be a useful control technique to counteract the downstream deformation of the shock caused by an expansion wave originating at the engine. The computed total energy and density for the perfect gas and real gas models are similar.

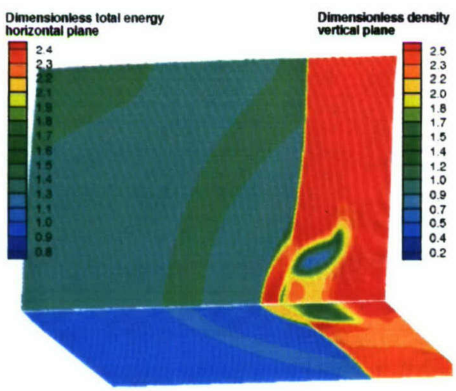


Fig. 14 Total energy and density contours for perfect gas model

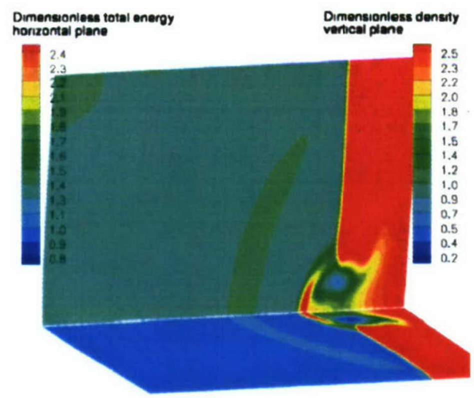


Fig. 15 Total energy and density contours for real gas model

Tests were conducted in the Mach 1.4 supersonic wind tunnel facility at UIUC to investigate the interaction of laser induced optical breakdown with a normal shock. The normal shock train was stabilized in the tunnel by regulating the stagnation pressure. The laser beam used to create the laser spark was focused in the middle of the supersonic flow before the first normal shock, at the normal shock, and near within the lower wall boundary layer. Fig. 16 shows phased average schlieren images of laser energy deposition in a normal shock train for the upstream excitation location. The formation of the hot laser spark and growing blast wave are clearly observed, and both flow features convect downstream. As the heat region interacts with the normal shock, the shock moves upstream (the "lensing" effect), and a vortex ring and induced jet are created due to the shock curvature. Similar trends are observed in the computational investigation of this flow field performed earlier[5].

---

[5] Yan, H., Knight, D., Kandala, R. and Candler, G., "Control of Normal Shock by a Single Laser Pulse", AIAA Paper No. 2004-2126, June 2004; Yan, H., Knight, D., and Elliott, G., "Numerical Study of Control of Normal Shock by Energy Pulse", AIAA Paper No. 2005-0785, January 2005

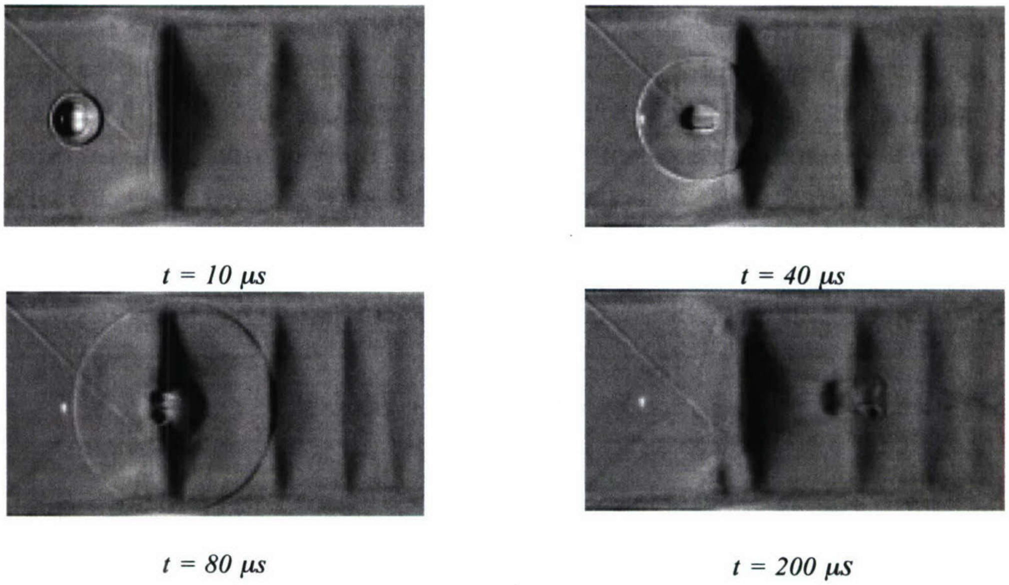


Fig. 16. Phase averaged schlieren images of laser energy deposition interaction with normal shock train.

### *IV.B Local Flow Control of Supersonic Flow Over a 3-D Cavity*

Tests were conducted in the Mach 1.4 supersonic wind tunnel facility at UIUC to investigate the effect of pulsed energy deposition on the shear layer (either enhancing or destroying large scale structures depending on the application) over a 3-D cavity and/or pressure waves inside the cavity. By utilizing a combination of spherical and cylindrical lenses, a short spanwise line can be formed at the upstream edge of the cavity. Fig. 17 shows phase average schlieren images taken 150 μs after the initiating laser pulse and the same shear layer with no excitation. Two flow phenomena are observed: the blast wave which grows from the focal point and large scale structures in the shear layer which convect downstream. It is noted that the blast wave and large scale structures may or may not be desirable depending on the application. For example, large scale structures may be particularly attractive for mixing fuel and air in propulsion applications.

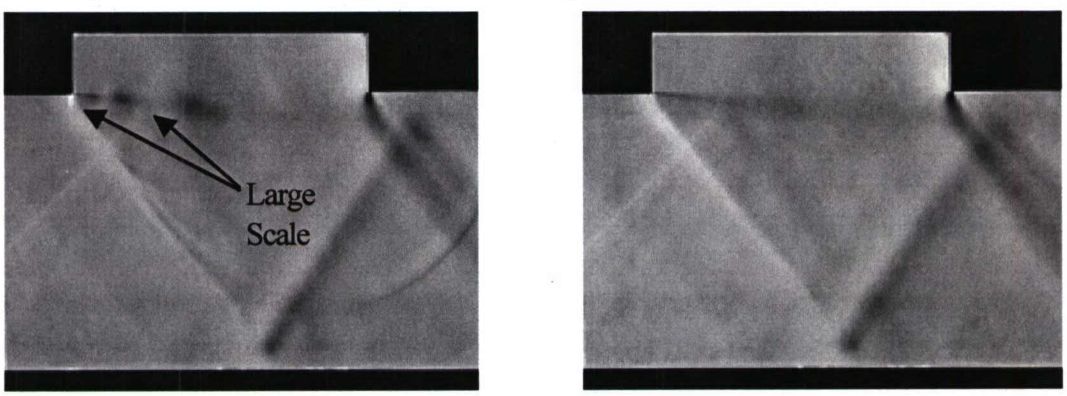


Fig. 17. Phase averaged schlieren images of the shear layer below a Mach 1.4 supersonic cavity occurring 150 μs (a) after spanwise excitation and with no forcing (b).

### *IV.C Control of Vortex Breakdown in Supersonic Flow*

The interaction of a supersonic vortex with a shock wave (*e.g.*, on the upper surface of a wing) can result in vortex breakdown and, if the breakdown occurs on one wing only, a large roll moment for the aircraft. Adequate roll control authority may not be available under certain conditions thereby resulting in loss of aircraft stability. A plausible control strategy is to force symmetric vortex breakdown to avoid the high roll moment.

The capability for control of vortex breakdown by localized steady and pulsed energy deposition during interaction of the vortex with an oblique shock wave at Mach 3 and 5 has been examined using a perfect gas model. A series of three-dimensional simulations were performed for a range of energy levels and shock strengths. For sufficiently high energy level, a subsonic wake is formed behind the energy deposition region and causes a significant increase in the size recirculation zone (Fig. 18). Increased unsteadiness was observed at the early stages of vortex breakdown for pulsed energy deposition.

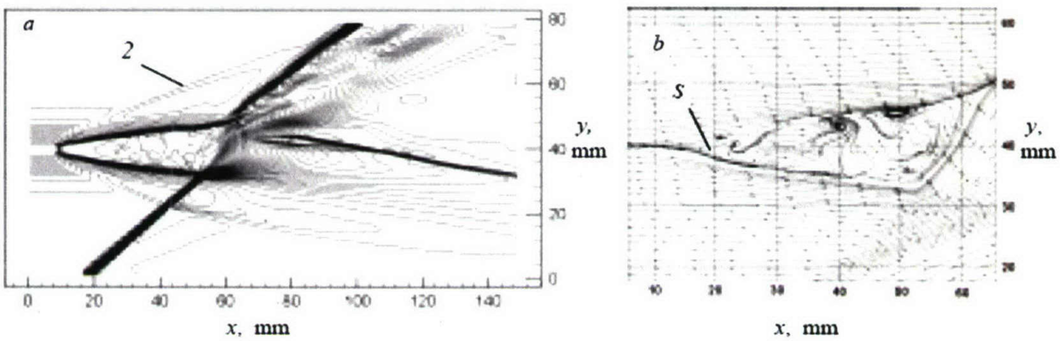


Fig. 18 Vortex-shock interaction with steady energy deposition at Mach 3

### *IV.D Local Flow Control of Edney IV Interaction*

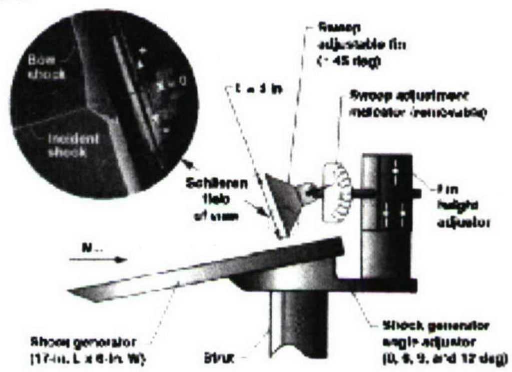


Fig. 19 Experimental configuration

A preliminary computational study was performed to examine the capability of pulsed laser energy deposition for control of the high localized pressure and heat flux in an Edney IV interaction. The configuration (Fig. 19) is a swept fin with an impinging shock wave. and represents an Edney IV interaction on a high speed inlet cowl. A single location for the pulsed laser energy deposition was considered. The flowfield is modeled with tools developed earlier in this program. First, the undisturbed flowfield is obtained with a conventional CFD method. Next, our laser energy deposition model is used to determine the conditions of the laser spark. Typically, this simulation is carried out for the 10 ns duration of laser operation until about 50 μs. The resulting flowfield is then superimposed on the undisturbed flow, and a time-accurate calculation is performed. The surface pressure distribution and heat flux are monitored as the heated gas moves past the wind tunnel model. Fig. 20 displays the maximum surface pressure and heat flux as a function of time during the simulated interaction, with the undisturbed maximum values used to normalize the results. Also shown are two snapshots of the flowfield in the plane of the centerline of the swept fin. Note that, for the single energy deposition location considered, the surface quantities are substantially increased above their undisturbed values. The high temperature region causes the shock interaction to collapse and form a very high pressure and temperature region that impinges on the leading edge of the fin (Fig. 20).

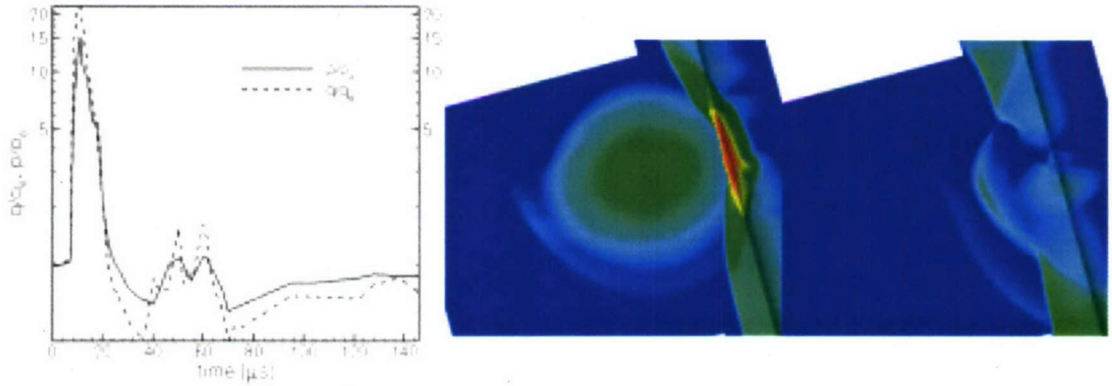


Fig. 20 Maximum surface pressure and heat flux normalized by maximum values in undisturbed flow (left); and pressure fields at two times during the interaction of the heated region with the swept fin (right).


**Acknowledgment/Disclaimer**

This work was sponsored (in part) by the Air Force Office of Scientific Research, USAF, under grant/contract number FA9550-04-1-0177. The views and conclusions contained herein are those of the authors and should not be interpreted as necessarily representing the official policies or endorsements, either expressed or implied, of the Air Force Office of Scientific Research or the U.S. Government.


**Personnel Supported During Duration of Grant**

| | |
|---|---|
| Graham Candler | Professor, University of Minnesota |
| Greg Elliott | Associate Professor, University of Illinois |
| Nick Glumac | Associate Professor, University of Illinois |
| Ramnath Kandala | Graduate Student, University of Minnesota |
| Doyle Knight | Professor, Rutgers University |
| Eli Lazar | Graduate Student, University of Illinois |
| Taylor Swanson | Graduate Student, University of Illinois |
| Kerry Trumble | Graduate Student, University of Minnesota |
| Hong Yan | Research Asst Professor, Rutgers University |

**Publications**

1. "Measurements in Fluid Flows Using Molecular Filter-based Techniques", M. Boguszko, G. Elliott, AIAA Paper No. 2004-0018, January 2004.
2. "Energy Deposition in Supersonic Cavity Flow", S. Aradag, H. Yan, D. Knight, AIAA Paper No. 2004-0514, January 2004.
3. "Computational Simulation of Laser-Induced Plasmas for Supersonic Flow Control", R. Kandala, G. Candler, AIAA Paper No. 2004-0989, January 2004.
4. "Survey of Magneto-Gasdynamic Local Flow Control at High Speeds", D. Knight, AIAA Paper No. 2004-1191, January 2004.
5. "Control of Normal Shock by a Single Laser Pulse", H. Yan, D. Knight, R. Kandala, G. Candler, AIAA Paper No. 2004-2126, June 2004.
6. "Streamwise Vortex/Shock Wave Interaction in Energy Deposition Conditions", A. Zheltovodov, E. Pimonov, International Conference on Methods of Aerophysical Research, June 2004.
7. "Numerical Studies of Laser-Induced Energy Deposition for Supersonic Flow Control", Kandala, R., and G.V. Candler, *AIAA Journal*, Vol. 42, No. 11, pp. 2266-2275, Nov. 2004.
8. "Control of Edney IV Interaction by Pulsed Laser Energy Deposition", Adelgren, R., Yan, H., Elliott, G., Knight, D., Beutner, T. and Zheltovodov, A., *AIAA Journal*, Vol. 43, No. 2, 2005, pp. 256-269.
9. "Temporal and Spatial Evolution of the Thermal Structure of a Laser Spark in Air", Glumac, N., Elliott, G., and Boguszko, M., AIAA Paper No. 2005-0204, January 2005.
10. "Simulation of Laser-Induced Plasma Experiments for Supersonic Flow Control", Kandala, R., Candler, G., Glumac, N., and Elliott, G., AIAA Paper No. 2005-0205, January 2005.
11. "Numerical Study of Control of Normal Shock by Energy Pulse", Yan, H., Knight, D. and Elliott, G., AIAA Paper No. 2005-0785, January 2005.
12. "Simulation of Supersonic Flow Over a Cavity", Aradag, S. and Knight, D., AIAA Paper No. 2005-0848, January 2005.
13. Zheltovodov, A., Pimonov, E. and Knight, D., "Supersonic Vortex Breakdown Control by Energy Deposition", AIAA Paper No. 2005-1048, January 2005.
14. Kandala, R., "Numerical Simulations of Laser Energy Deposition for Supersonic Flow Control", PhD Thesis, Aerospace Engineering and Mechanics, University of Minnesota, April 2005.
15. Zheltovodov, A., Pimonov, E. and Knight, D., "Vortex Breakdown Control by Energy Deposition in High Speed Flows", Sixth Workshop on Magnetoplasma Aerodynamics for Aerospace Applications, Moscow, Russia, May 24-27, 2005.
16. Knight, D., Yan, H., Candler, G., Kandala, R., Zheltovodov, A. and Pimonov, E., "Control of Normal Shock by Pulsed Energy Deposition", Sixth Workshop on Magnetoplasma Aerodynamics for Aerospace Applications, Moscow, Russia, May 24-27, 2005.

17. Kandala, R. and Candler, G., "Numerical Studies of Laser-Induced Energy Deposition for Supersonic Flow Control", 3rd MIT Conference on Computational Fluid and Solid Mechanics, June 2005.
18. Pimonov, E., Zheltovodov, A. and Knight, D., "Research of Shock Wave-Induced Vortex Breakdown Control by Energy Deposition", European Conference for Aerospace Sciences (EUCASS), Moscow, Russia, July 4-7, 2005.
19. Knight, D., Yan, H., Candler, G., Kandala, R., Elliott, G., Glumac, N., Zheltovodov, A. and Pimonov, E., "High Speed Flow Control Using Pulsed Energy Deposition", European Conference for Aerospace Sciences (EUCASS), Moscow, Russia, July 4-7, 2005.
20. Glumac, N., Elliott, G.S., and Boguszko, M., "Temporal and Spatial Evolution of the Thermal Structure of a Laser Spark in Air," *AIAA Journal*, Vol. 43, No. 9, pp. 1984-1994, 2005.
21. Glumac, N., and Elliott, G., "The Effect of Ambient Pressure on Laser-Induced Plasmas in Air," AIAA Paper 2006-0399, January 2006.
22. Zheltovodov, A., Pimonov, E. and Knight, D., "Vortex Breakdown Simulation by the Steady and Periodic Pulse Energy Deposition in a Vicinity of Shock Wave", AIAA Paper No. 2006-0401, January 2006.
23. Trumble, K. and G.V. Candler, "Flow Control of Swept Fin Shock Interactions by Laser-Induced Plasmas," AIAA 2006-0405, January 2006.
24. Khmara, D., Kolesnichenko, Y. and Knight, D., "Modeling of Microwave Filament Origination", AIAA Paper No. 2006-0794, January 2006.
25. Aradag, S., "A Critical Evaluation of Numerical Algorithms and Flow Physics in Complex Supersonic Flows", PhD Thesis, Department of Mechanical and Aerospace Engineering, Rutgers University, May 2006.
26. Khmara, D., Kolesnichenko, Y., and Knight, D., "A Kinetic Model of Microwave Energy Deposition in Air", Fifth Workshop on Thermochemical Processes in Plasma Aerodynamics, St. Petersburg, Russia, June 2006.
27. Knight, D., Yan, H., Swanson, T., Elliott, G. and Glumac, N., "Interaction of Pulsed Energy Deposition with a Normal Shock: Experimental and Computational Investigation", Fifth Workshop on Thermochemical Processes in Plasma Aerodynamics, St. Petersburg, Russia, June 2006.
28. Glumac, N., and Elliott, G.S., "The Effect of Ambient Pressure on Laser-Induced Plasmas in Air," *Optics and Lasers in Engineering*, Vol. 45, No. 1, 2007, pp. 27-35.
29. Yan, H., Knight, D., Kandala, R. and Candler, G., "Effect of a Laser Pulse on a Normal Shock", accepted for publication in *AIAA Journal*.